Active Control of Rogue Waves for Stimulated Supercontinuum Generation

D. R. Solli,[1] C. Ropers,[1,2] and B. Jalali[1]

[1]*Department of Electrical Engineering, University of California, Los Angeles, California 90095, USA*
[2]*Courant Research Center Nano-Spectroscopy and X-Ray Imaging, University of Göttingen, Göttingen, Germany*
(Received 5 August 2008; published 5 December 2008)

We demonstrate that rogue waves provide a powerful tool to actively control a nonlinear system with minimal effort. Specifically, optical rogue waves—rare, bright flashes of broadband light arising in subthreshold supercontinuum generation—are initiated by an exceedingly weak stimulus. Using this effect, we produce an optically switchable, ultrastable, and bright supercontinuum with greatly enhanced coherence.

Nonlinear processes, often noted for their counterintuitive hallmark, have occupied a central role in physics during the past half century. Especially in optics, the availability of high-intensity, short pulses of coherent radiation have brought nonlinear effects to center stage. A particularly striking example of nonlinear action in optics is supercontinuum (SC) generation, a process in which extremely broadband radiation is generated from narrow band light through a concert of optical nonlinearities. First discovered in the late 1960s by Alfano and Shapiro [1], SC light differs markedly from the white light produced by an ordinary light bulb because it can be far brighter, more coherent, and directional, resulting in many applications in research and technology [1,2].

Because of their complexities, many nonlinear systems continue to harbor surprises. For example, optical rogue waves—statistically rare bursts of white light counterpart to oceanic freak waves—are produced in SC generation accelerated by a specific type of noise in the input light [3]. Described by so-called *L*-shaped probability distributions, extreme waves are rare, but much more common than expected from Gaussian statistics. Amazingly, this tremendous variability generally arises from nearly indistinguishable initial conditions, indicating that minute perturbations can have tremendous repercussions [3,4]. If regulated experimentally, the "rogue wave instability" could have great scientific and practical utility, both in optics and in other systems displaying rogue behavior.

Optical rogue waves testify to the significant role of noise in SC generation. Even in less extreme examples, noise has a serious impact, degrading SC stability through spectral fluctuations, loss of coherence, and other forms of jitter [2,5–7]. These instabilities negatively impact many important applications of SC, such as optical frequency metrology [8], generation of ultrashort optical pulses [2], photonic time stretch analog-to-digital conversion [9], and optical coherence tomography [10].

A multitude of nonlinear optical effects contribute to the generation of SC, and their relative contributions depend strongly on the experimental conditions [2]. The primary method for producing ultrabroadband SC involves the so-

called soliton-fission mechanism, a process that occurs when intense pump pulses are launched into a nonlinear optical fiber at its zero-dispersion wavelength [11]. In this situation, the input light fissions into multiple solitons— nonlinear wave packets that propagate without spreading due to a balance between dispersion and nonlinearity [12]—at different redshifted wavelengths, along with blue-shifted dispersive radiation [11].

At the heart of soliton-fission based SC generation is a nonlinear growth process known as modulation instability (MI) [12]. This effect adds sidebands to narrow band input radiation that increase the optical bandwidth of the input pulse until the Raman-induced self-frequency shift [12] can separate it into redshifted solitons [13–15]. Because the MI growth starts spontaneously from noise [16], the subsequent initiation of soliton fission becomes inherently unpredictable [2]. Particularly for longer input pulses, much of the initial spectral broadening preceding soliton fission is spontaneously initiated by either shot noise, spontaneous emission, or other source fluctuations [2]; as a result, the resulting SC can become incoherent away from the pump wavelength, and is subject to large pulse-to-pulse variations [2,5,14,17]. Below the power threshold for soliton fission, this variability can be so extreme that optical rogue waves arise [3].

Here, we demonstrate that the rogue wave instability can be actively controlled to enhance and becalm SC generation. By applying a tailored, but extremely weak coherent pulse, we exploit the rogue wave instability, stimulating SC generation by initiating modulation instability with a controlled signal rather than noise. This minute stimulation or seed pulse ($10\,000\times$ weaker than the pump) lowers the input pump power threshold for SC generation, and dramatically reduces the instability of the resulting white light relative to the spontaneous SC above threshold. Using spectral interferometry and real-time measurements, we show that the stimulated SC has high coherence and low intensity noise. In the past, induced MI has been used to generate high-repetition rate trains of soliton pulses [18], promote the formation of Raman solitons [19,20], and produce a MI-soliton laser [21]; however, the enhancement

and stabilization of SC generation with a weak stimulus has not yet been demonstrated. This process possesses many of the striking advantages attributed to stimulated effects, such as increased intensity stability and phase coherence.

Conventional (unseeded) SC generation with pulses of picosecond duration is a spontaneous, largely uncontrolled process occurring above a certain power threshold [2], and subthreshold pump pulses generate only rare, random flashes of SC radiation [3]. In contrast, seeding the process causes the once rare events to become the norm, and induces a drastic transition in the SC's noise characteristics. In our experiments, we employ a timed, frequency-shifted, weak seed pulse, which lowers the SC power threshold by more than 25%. Remarkably, it reduces fluctuations of the power spectral density by 90%, and also induces significant pulse-to-pulse coherence in the output light, which is absent in the unseeded SC. In addition, the method allows broadband optical switching with a dynamic range of 30 dB, actuated by a weak field.

Picosecond pump pulses from a mode-locked laser ($\lambda = 1550$ nm) are amplified, filtered ($\sim$1 nm bandwidth), and delivered to a highly nonlinear optical fiber ($L = 15$ m, Corning HNL ZD 1550) with very low dispersion at 1550 nm. The pump pulses are $\sim$3.7 ps in duration, as determined by autocorrelation. A weak seed pulse (0.01% of the pump intensity) derived from the same source, but with a shifted center frequency ($\sim$1630 nm), is produced by broadening a portion of the laser output and filtering the result. This seed pulse is precisely timed and coupled to the highly nonlinear fiber along with the pump. As illustrated schematically in Fig. 1(a), the output light depends dramatically on the timing of the weak stimulus.

In Fig. 1(b) we show the output spectra measured with an optical spectrum analyzer for pump power levels below and above threshold without the proper timing of the stimulus. Below threshold, the central portion of the spectrum shows the characteristic undulations of self-phase modulation (SPM) (fine oscillations on the central peak), along with broad MI wings. As the input power is increased, the power within the MI lobes increases until a soliton is ejected from the red lobe. This point marks the beginning of soliton fission. When the stimulus is not properly timed, it has essentially no effect; however, the situation changes dramatically when it is properly timed with the pump [cf. Fig. 1(c)]. The MI lobes sharpen, and the power threshold for soliton fission is reduced.

These spectra clearly show that SC generation is significantly accelerated by an extremely weak seed pulse. To quantify the spectral width of the SC, we carve out a portion ($\lambda = 1685$ nm, $\Delta\lambda = 10$ nm) beyond the red edge of the seed spectrum. We monitor the output power within this wavelength band as a function of the pump power, with and without the properly timed stimulus. Figure 2(a) shows that the redshifted output exhibits a sharp transition threshold, which is reduced by the stimulation. Although it is 10 000× weaker than the pump, the
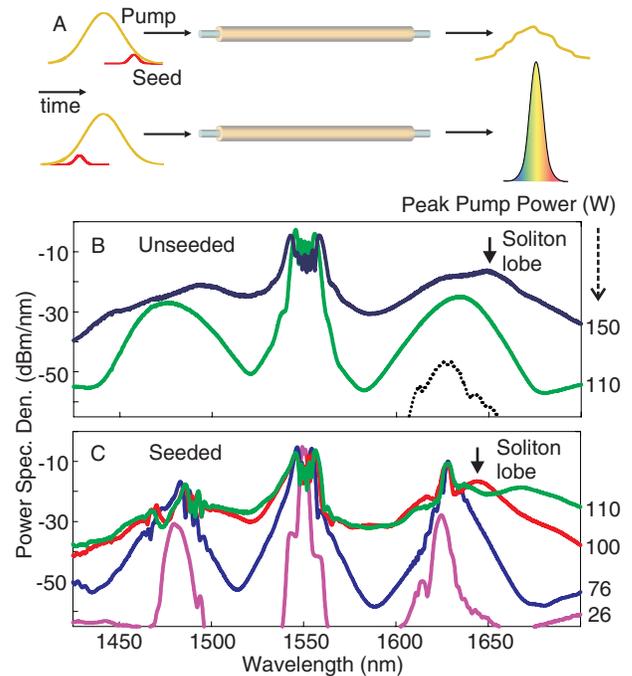

FIG. 1 (color online). (a) Illustration of the impact of a weak stimulus on the input pulse. With proper timing and frequency, SC is produced (bottom), whereas SC is not generated otherwise (top). (b),(c) Measured spectra without and with the proper stimulus, respectively, at the indicated power levels. Small arrows indicate soliton shedding from the MI wing, clearly discernible when the stimulation is present.

seed creates a power contrast of 30 dB. In other words, selective application of the weak, narrow band stimulus can be used to switch the SC on and off (as a new type of optical transistor or three-terminal device), a feature that is unique to the present approach for generating SC.

Next, we use a real-time detection technique to directly measure the impact of the seed on the pulse-to-pulse spectral fluctuations of the SC. Group-velocity dispersion is used to stretch the pulses so that a large number can be captured with a photodetector and a single-shot oscilloscope in real time; this method was also recently used to identify optical rogue waves [3]. Whereas a stable stimulus is not needed to simply lower the threshold for SC generation, its stability is essential for producing stable stimulated SC. Figure 2(b) compares the statistical histograms of bandpass-filtered SC pulses with and without the properly timed stimulus. This measurement shows a dramatic 90% reduction in the standard deviation of pulse-to-pulse intensity variations in the stimulated SC. Furthermore, the fluctuations clearly depend on the relative delay between the pump and seed [cf. Fig. 2(b), inset]: when the stimulus is not present only rogue SC pulses are produced. We expect that even greater stability can be achieved with this approach if the current limitations from residual seed fluctuations are reduced.

The lack of pulse-to-pulse coherence is currently one of the major drawbacks of many existing SC sources gener-
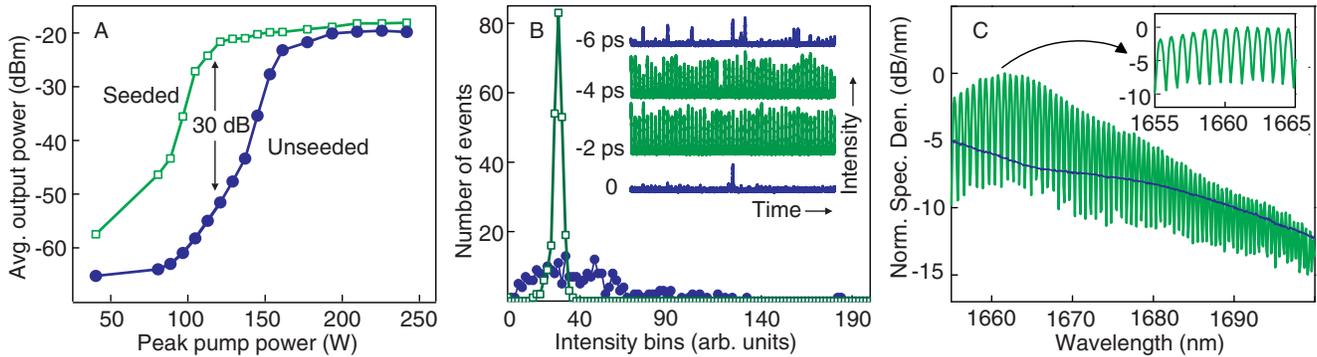
FIG. 2 (color online).   (a) Measured (filtered) SC power with and without the seed. (b) Measured (filtered) SC pulse-to-pulse intensity statistics with (green) and without (blue) the stimulus (~ 100 events each). Pump power is adjusted ($P_{pump} \approx 130$ W stimulated, ≈ 200 W spontaneous) to keep average SC output power constant. Inset illustrates segments of the filtered SC pulse train for different seed delay. Negative time corresponds to advanced seed. (c) Measured spectral interferograms of a coherently stimulated SC (green trace) and a conventional, spontaneous SC (blue trace). Fringes are visible only for the seeded SC.

ated from picosecond pump pulses. This limitation can be overcome by the stimulation process. Pulse-to-pulse coherence represents the ability of two light pulses to interfere with each other. The interference appears as fringes in the optical spectrum when consecutive pulses are overlapped with a slight temporal delay, and the fringe contrast, when averaged over many pulse pairs, reflects the degree of coherence. Spontaneous SC is virtually incoherent, and cannot produce interference fringes, because there is no pulse-to-pulse correlation in the noise that initiates the soliton-fission process. When coherently stimulated, however, the interferogram exhibits high-contrast fringes [cf. Fig. 2(c)] because the seeding produces waveforms with excellent pulse-to-pulse coherence. As the pump power is increased, the coherence gradually drops (sensitivity to seed fluctuations and noise heightens), but as shown, high pump power is not required to produce stimulated SC.

We also numerically model seeded SC generation. The generalized nonlinear Schrödinger equation (NLSE) includes the effects of dispersion, the Kerr nonlinearity, and Raman scattering [12]. Using the NLSE, we calculate the SC spectrum as a function of the relative time delay and frequency shift between the pump and seed pulses, and quantify the amount of broadening by the redshifted energy (cf. Fig. 3). In this calculation, the pump pulse has insufficient power to generate SC without the stimulus. The maps of Fig. 3 exhibit a "sensitive spot" in which the perturbation has powerful impact. Outside of this region, its effect is negligible by comparison.

One may wonder why the input pulse is most sensitive to a specific perturbation. A previous study has observed that MI can lead to the growth of disturbances on the steep regions of a pulse envelope [13]; however, under their conditions, growth appeared on both sides of the envelope, and the initial formation was attributed to frequency beating. In the present situation, the initial modifications to the pump field originate primarily from the Kerr nonlinearity, which produces SPM and MI. SPM downshifts and upshifts the carrier frequency on its leading and trailing

slopes, respectively, where the intensity changes rapidly [12]. This produces a broadened, chirped pulse, straddling the zero-dispersion wavelength. The trailing edge, now in the normal dispersion regime, does not produce MI; however, the leading edge moves into the fiber's anomalous dispersion regime, driving MI with a frequency shift that reduces as the redshift increases. When the MI shift is large, dispersion causes rapid "walk-off" of the MI growth from the appropriate region of the pump, limiting the total gain.

The interplay creates a special region on the pump envelope where the instantaneous MI gain is large enough and the walk-off is not too rapid. A properly timed stimulus with a frequency matching the MI shift of this special region experiences the largest cumulative MI gain. Once the MI growth becomes large enough, soliton fission begins suddenly as a large disturbance, traveling much slower than the remnants of the original envelope. This disturbance rapidly disintegrates the original pulse shape, and liberates one or more narrow solitons while leading to rapid spectral broadening. Without the seed, soliton fission will occur if the pump power is large enough; however, the process begins rather suddenly and explosively (somewhat like the onset of boiling in a superheated liquid), typically fissioning into multiple solitonic pulses. On the other hand,
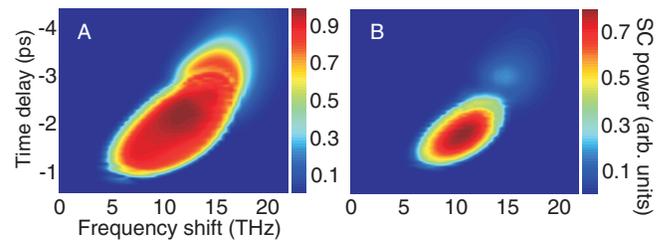

FIG. 3 (color online).   SC power integrated over redshifted wavelengths (>1680 nm) as a function of the time delay and frequency shift of the seed pulse for intensities: (a) 0.01% and (b) 0.001% of pump. Negative time corresponds to the pump's leading edge. $P_{pump} = 130$ W, $\tau_{pump} = 3.7$ ps, $\tau_{seed} = 200$ fs.
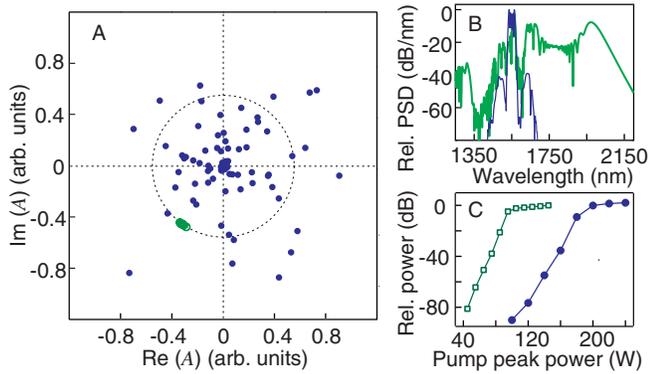
FIG. 4 (color online). (a) Complex-plane scatter plot of the SC electric field amplitude ($\lambda = 1950$ nm, $\Delta\lambda = 5$ nm) from many independent events: 130 W pump peak power, stimulated (green, tightly clustered on dotted circumference); 255 W, spontaneous (blue, scattered). Although SC average power is comparable for both cases, fluctuations are nearly eliminated with seeding (magnitude, $CV = 0.036\%$; phase, $\sigma = 23$ mrad). (b) Single-shot stimulated (green) and spontaneous (blue) relative power spectral densities from 130 W pump. (c) Filtered (>1680 nm) SC power with (green squares) and without (blue circles) seeding.

with stimulation, a less intense pump produces a single soliton at an earlier stage.

We also model the impact of the stimulation on the SC spectrum, threshold, intensity fluctuations, and phase coherence. We include the effects of input noise by adding a small amount of bandwidth-limited ($\sim$30 THz) random noise to its envelope (noise amplitude proportional to instantaneous field strength). We choose the overall noise amplitude so that the threshold is similar to that in the experiment without the stimulus. To illustrate the impact of the stimulus on both the intensity stability and coherence, we present a complex-plane scatter plot of the redshifted electric field from many independent events [cf. Fig. 4(a)]. Although the spontaneous SC produces large scatter, the stimulated events are nearly identical. Figure 4(b) shows typical single-shot SC spectra with and without the seed at a fixed pump power. By varying the input pump power, we also calculate the stimulated and spontaneous SC thresholds [cf. Fig. 4(c)].

We point out that high-power pulses are capable of producing coherent SC in bulk media [22]: without MI, the SC is fairly insensitive to noise. In the zero or anomalous dispersion regime, which typically permits larger broadening factors (output to input bandwidth ratio), ultrashort pulses ($\sim$10 fs) are also capable of producing coherent SC. For such pulses, the initial bandwidth is great enough to seed MI by the tail of the spectrum [2]. Much larger broadening factors can be realized with narrow band input pulses, indicating large effective nonlinearity, but stability is sacrificed [23]. In contrast, the present approach preserves coherence, while maintaining very large broadening factors. Specialized methods can also be used to

reduce excess noise with SC generation from longer pulses [5,15,24]; however, the present approach uniquely offers a means to actively regulate the generation process with a third terminal. Active control may also benefit SC generation with shorter pulses.

In conclusion, rogue waves reveal a means to exert maximal control over a nonlinear system with minimal effort. We have applied this effect to produce highly stable SC. Just below the SC threshold, very little white light average power is generated, although short, rare bursts of intense white light—optical rogue waves—may be spontaneously emitted due to accidental seeding of MI by noise. On the other hand, a weak perturbation can cause intense SC pulses to become the stable norm. As an ultrafast broadband optical switch, optically triggered SC, and stable SC source, this effect has significant potential for applications. For example, it could be used for data switching and routing in optical networks. Finally, we point out that this effect may also be useful in influencing the dynamics of other nonlinear systems.

[1] R. R. Alfano, Sci. Am. **295**, No. 6, 86 (2006).
[2] J. M. Dudley, G. Genty, and S. Coen, Rev. Mod. Phys. **78**, 1135 (2006).
[3] D. R. Solli *et al.*, Nature (London) **450**, 1054 (2007).
[4] J. M. Dudley, G. Genty, and B. J. Eggleton, Opt. Express **16**, 3644 (2008).
[5] H. Kubota, K. R. Tamura, and M. Nakazawa, J. Opt. Soc. Am. B **16**, 2223 (1999).
[6] A. L. Gaeta, Opt. Lett. **27**, 924 (2002).
[7] K. L. Corwin *et al.*, Phys. Rev. Lett. **90**, 113904 (2003).
[8] B. R. Washburn and N. R. Newbury, Opt. Express **12**, 2166 (2004).
[9] Y. Han and B. Jalali, J. Lightwave Technol. **21**, 3085 (2003).
[10] D. L. Marks *et al.*, Opt. Lett. **27**, 2010 (2002).
[11] J. Herrmann *et al.*, Phys. Rev. Lett. **88**, 173901 (2002).
[12] G. P. Agrawal, *Nonlinear Fiber Optics* (Academic, San Diego, 2007), 4th ed.
[13] M. Nakazawa *et al.*, Phys. Rev. A **39**, 5768 (1989).
[14] M. N. Islam *et al.*, J. Opt. Soc. Am. B **6**, 1149 (1989).
[15] J. N. Kutz, C. Lyngå, and B. J. Eggleton, Opt. Express **13**, 3989 (2005).
[16] S. B. Cavalcanti, G. P. Agrawal, and M. Yu, Phys. Rev. A **51**, 4086 (1995).
[17] F. Vanholsbeeck *et al.*, Opt. Express **13**, 6615 (2005).
[18] K. Tai *et al.*, Appl. Phys. Lett. **49**, 236 (1986).
[19] A. S. Gouveia-Neto, M. E. Faldon, and J. R. Taylor, Opt. Lett. **13**, 1029 (1988).
[20] P. V. Mamyshev *et al.*, Opt. Lett. **15**, 1365 (1990).
[21] M. Nakazawa, K. Suzuki, and H. A. Haus, IEEE J. Quantum Electron. **25**, 2036 (1989).
[22] M. Bellini and T. W. Hänsch, Opt. Lett. **25**, 1049 (2000).
[23] J. N. Ames *et al.*, Appl. Phys. B **77**, 279 (2003).
[24] Ö. Boyraz *et al.*, J. Lightwave Technol. **18**, 2167 (2000).